SF2A 2012
S. Boissier, P. de Laverny, N. Nardetto, R. Samadi, D. Valls-Gabaud and H. Wozniak (eds)

CHARRON: CODE FOR HIGH ANGULAR RESOLUTION OF ROTATING OBJECTS IN NATURE*

A. Domiciano de Souza[1], J. Zorec[2] and F. Vakili[1]

Abstract. Rotation is one of the fundamental physical parameters governing stellar physics and evolution. At the same time, spectrally resolved optical/IR long-baseline interferometry has proven to be an important observing tool to measure many physical effects linked to rotation, in particular, stellar flattening, gravity darkening, differential rotation. In order to interpret the high angular resolution observations from modern spectro-interferometers, such as VLTI/AMBER and VEGA/CHARA, we have developed an interferometry-oriented numerical model: CHARRON (Code for High Angular Resolution of Rotating Objects in Nature). We present here the characteristics of CHARRON, which is faster ($\simeq 10-30$ s per model) and thus more adapted to model-fitting than the first version of the code presented by Domiciano de Souza et al. (2002).

Keywords: Stars: rotation, Methods: observational, Methods: numerical, Techniques: interferometric, Techniques: high angular resolution

1 Introduction

Many recent observations and theories show that rotation (or angular momentum) is a key ingredient in stellar physics (e.g. Maeder & Meynet 2012; van Belle 2012; Maeder & Meynet 2000). Rotation modifies several aspects of the stellar physical structure (geometircal shape, temperature and luminosity distribution, convective and radiative zones, etc) and evolution (lifetimes, evolutionary tracks, chemical abundances, final stellar masses, rotation periods of pulsars).

Since the beginning of the 21st century, optical/IR long-baseline spectro-interferometry (OLBSI) has been providing crucial observations that greatly improve our understanding of rotating stars. By spatially resolving the stellar surface, OLBSI directly proved that fast rotating stars are flattened (rotationally distorted photospheres; e.g. van Belle et al. 2001; Domiciano de Souza et al. 2003) and and gravity darkened (poles hotter than the equator; e.g. Domiciano de Souza et al. 2005; Che et al. 2011). These important results were obtained from spectro-interferometric observables like visibility amplitudes and closure phases. Recently, Domiciano de Souza et al. (2012)showed that the differential phases (an still under-exploited observable) allow to measured measure angular diameters, rotation velocities, and orientation of stellar rotation axes.

In order to interpret the OLBSI observations and constraint the physical parameters of rotating stars, it is important to develop models including the main physical effects caused by high rotation rates. In this work we describe the IDL-based model CHARRON[i] (Code for High Angular Resolution of Rotating Objects in Nature), which is dedicated to the interpretation and analysis of spectro-interferometric observations of rotating stars.

2 Basic equations of stellar rotation

As discussed by Zorec et al. (2011), the gravitational potential of rotating centrally condensed objects is, in most realistic cases, well described (better than $\sim 5\%$) by a simple central-field expression (Roche approximation):

$$\Phi_{\rm G}(\theta) = -GM/R_{\rm s}(\theta) \ , \tag{2.1}$$

[1] Laboratoire J.-L. Lagrange, UMR 7293, OCA-UNS-CNRS, Boulevard de l'Observatoire, BP 4229, 06304 Nice Cedex 4, France
[2] UPMC Univ. Paris 06, UMR7095, Institut d'Astrophysique de Paris, 98bis Bd. Arago, 75014 Paris, France

[i]Name of an ancient profession (from Wikipedia french webpage: *spécialiste du bois, maître de tout ce qui tourne et roule, de la brouette à la charrette*).

where θ is the colatitude, $R_{\rm s}(\theta)$ is the stellar surface radius, and the other symbols have their usual meanings. This is equivalent to the potential that we would have if the whole mass was concentrated at the center of the star.

Many works showed the presence of differential rotation law in the surface of stars (e.g. Reiners & Royer 2004; Ammler-von Eiff & Reiners 2012; Zorec et al. 2012). Most of these works adopt a solar-like surface velocity (Maunder formula)

$$\Omega(\theta) = \Omega_{\rm e}(1 + \alpha \cos^2\theta) \ , \tag{2.2}$$

where $\Omega_{\rm e}$ is the equatorial angular velocity and α is the differential rotation parameter, corresponding to the excess of polar angular velocity ($\Omega_{\rm pol}$) relative to $\Omega_{\rm e}$, i.e., $\alpha = (\Omega_{\rm pol} - \Omega_{\rm e})/\Omega_{\rm e}$.

Equation 2.2 is a non-conservative rotation law, which implies that the shape of the star cannot be obtained from an effective rotational potential. It is instead defined from the surface resulting in a zero work done by the effective gravity $\mathbf{g}_{\rm eff}$ for an arbitrary displacement $d\mathbf{s}$ (Maeder 2009):

$$\mathbf{g}_{\rm eff} . d\mathbf{s} = 0 \ . \tag{2.3}$$

From the equation above and following Zorec et al. (2011), the surface of a star in the Roche approximation rotating with a Maunder-like non-conservative law is given by

$$\frac{R_{\rm s}(\theta)}{R_{\rm e}} = \frac{1}{1 + \eta_o[I(\pi/2) - I(\theta)]} \ , \tag{2.4}$$

where

$$I(\theta) = \frac{1}{2}\int_0^\theta \left[\frac{\Omega_{\rm s}(\theta)}{\Omega_{\rm e}}\right]^2 \left(\frac{d\varpi^2}{d\theta}\right) d\theta \ , \tag{2.5}$$

and

$$\varpi(\theta) = R_{\rm s}(\theta)\sin\theta \ . \tag{2.6}$$

The parameter η_o is the ratio of centrifugal to the gravitational acceleration in the equator

$$\eta_o = \frac{\Omega_{\rm e}^2 R_{\rm e}^3}{GM} \ . \tag{2.7}$$

The shape of the star $R_{\rm s}(\theta)$ is obtained by iteration using the equations above. Uniform rotation ($\Omega(\theta) = \Omega_{\rm e}$ constant) is a special case of this model, where shape of the star is given by the classical Roche model (e.g. Kopal 1987).

The surface effective gravity (gravitational plus centrifugal accelerations) is given by

$$\mathbf{g}_{\rm eff} = g_{{\rm eff},r}\hat{r} + g_{{\rm eff},\theta}\hat{\theta} = \left[-GM/R_{\rm s}^2(\theta) + \Omega(\theta)^2 R_{\rm s}(\theta)\sin^2\theta\right]\hat{r} + \left[\Omega(\theta)^2 R_{\rm s}(\theta)\sin\theta\cos\theta\right]\hat{\theta} \ . \tag{2.8}$$

The surface effective temperature is linked to $g_{\rm eff}$ through the gravity darkening effect (von Zeipel effect; von Zeipel 1924). We adopt the commonly used expression for the gravity darkening effect

$$T_{\rm eff}(\theta) = C_{\rm gd}\, g_{\rm eff}^{\beta}(\theta) \ , \tag{2.9}$$

where the gravity darkening parameter β depends on the surface temperature and internal physical conditions. The gravity darkening constant $C_{\rm gd}$ is obtained from

$$C_{\rm gd} = \left(\frac{\overline{T}_{\rm eff}^4 S}{\int g^{4\beta} ds}\right)^{1/4} = \left(\frac{L}{\sigma \int g^{4\beta} ds}\right)^{1/4} \ . \tag{2.10}$$

The stellar luminosity L, surface area S, and mean surface effective temperature are related by

$$L = S\sigma\overline{T}_{\rm eff}^4 \ , \tag{2.11}$$

σ being the Stefan-Boltzmann constant.

We note that in the equations above we are ignoring the Eddington factor, which changes the effective gravity but is significant only for very massive stars (above $\sim 20\ {\rm M}_\odot$).

3 CHARRON description and application example

The equations given in the previous section are implemented in CHARRON to define the physical structure of the rotating star in terms of shape, mass, luminosity, rotation rate, and local effective temperature and gravity. CHARRON is written in IDL[ii] and makes use of the fast vector operations provided by this language.

The numerical implementation of the physical equations and the discretization procedure of the stellar surface into thousands ($\simeq 50\,000$) small surface area elements are similar to those used in the code BRUCE (Townsend 1997) and in the interferometry-oriented code presented by Domiciano de Souza et al. (2002).

To obtain monochromatic intensity maps of the stellar photosphere a local spectrum, Doppler shifted by the local rotation velocity projected onto the observer's direction, is assigned each visible surface area element. This local photospheric spectrum, provided by the user, can be given as an analytical equation (including continuum, spectral line, limb darkening) or as the output of stellar atmosphere models calculated with radiative transfer codes. These local spectra can depend on different physical parameters, in particular the local effective temperature and gravity. CHARRON calculates the Fourier transform of the monochromatic intensity maps to obtain spectro-interferometric observables, in particular spectra, absolute and differential visibilities, differential phases, and closure phases.

A set of input parameters is required by CHARRON to define the stellar rotation model and spectro-interferometric observables. A useful set of input parameters is equatorial radius $R_{\rm e}$, equatorial rotation velocity $V_{\rm e}$, differential rotation parameter α, mass M, inclination i, distance d, gravity darkening parameter β, orientation of the rotation axis on the sky plane, and local profile.

Figure 1 shows examples of monochromatic intensity maps and differential phases $\phi_{\rm diff}(\lambda)$ of the fast rotating Be star Achernar calculated with CHARRON to interpret VLTI/AMBER $\phi_{\rm diff}(\lambda)$ observations of this star performed in the Br γ line at spectral resolution 12 000. The full results of the VLTI/AMBER data analysis and interpretation with CHARRON are given by Domiciano de Souza et al. (2012).

4 Conclusion and futur prospects

CHARRON, presented in this work, was shown to be well adapted to interpret spectro-interferometric observations of fast rotating stars. This code will be used to analyze the observations from several on-going observing programs on rotating stars, which have been proposed by our team on modern spectro-interferometers, in particular VLTI/AMBER and CHARA/VEGA.

References

Ammler-von Eiff, M. & Reiners, A. 2012, A&A, 542, A116

Che, X., Monnier, J. D., Zhao, M., et al. 2011, ApJ, 732, 68

Domiciano de Souza, A., Hadjara, M., Vakili, F., et al. 2012, A&A, 545, A130

Domiciano de Souza, A., Kervella, P., Jankov, S., et al. 2003, A&A, 407, L47

Domiciano de Souza, A., Kervella, P., Jankov, S., et al. 2005, A&A, 442, 567

Domiciano de Souza, A., Vakili, F., Jankov, S., Janot-Pacheco, E., & Abe, L. 2002, A&A, 393, 345

Kopal, Z. 1987, Ap&SS, 133, 157

Maeder, A. 2009, Physics, formation and evolution of rotating stars, 1st edn., Astronomy and Astrophysics Library (Springer-Verlag)

Maeder, A. & Meynet, G. 2000, ARA&A, 38, 143

Maeder, A. & Meynet, G. 2012, Reviews of Modern Physics, 84, 25

Reiners, A. & Royer, F. 2004, A&A, 415, 325

Townsend, R. H. D. 1997, MNRAS, 284, 839

van Belle, G. T. 2012, A&A Rev., 20, 51

van Belle, G. T., Ciardi, D. R., Thompson, R. R., Akeson, R. L., & Lada, E. A. 2001, ApJ, 559, 1155

von Zeipel, H. 1924, MNRAS, 84, 665

Zorec, J., Frémat, Y., Domiciano de Souza, A., et al. 2011, A&A, 526, A87

Zorec, J., Frémat, Y., Semaan, T., et al. 2012, submitted

[ii]Interactive Data Language

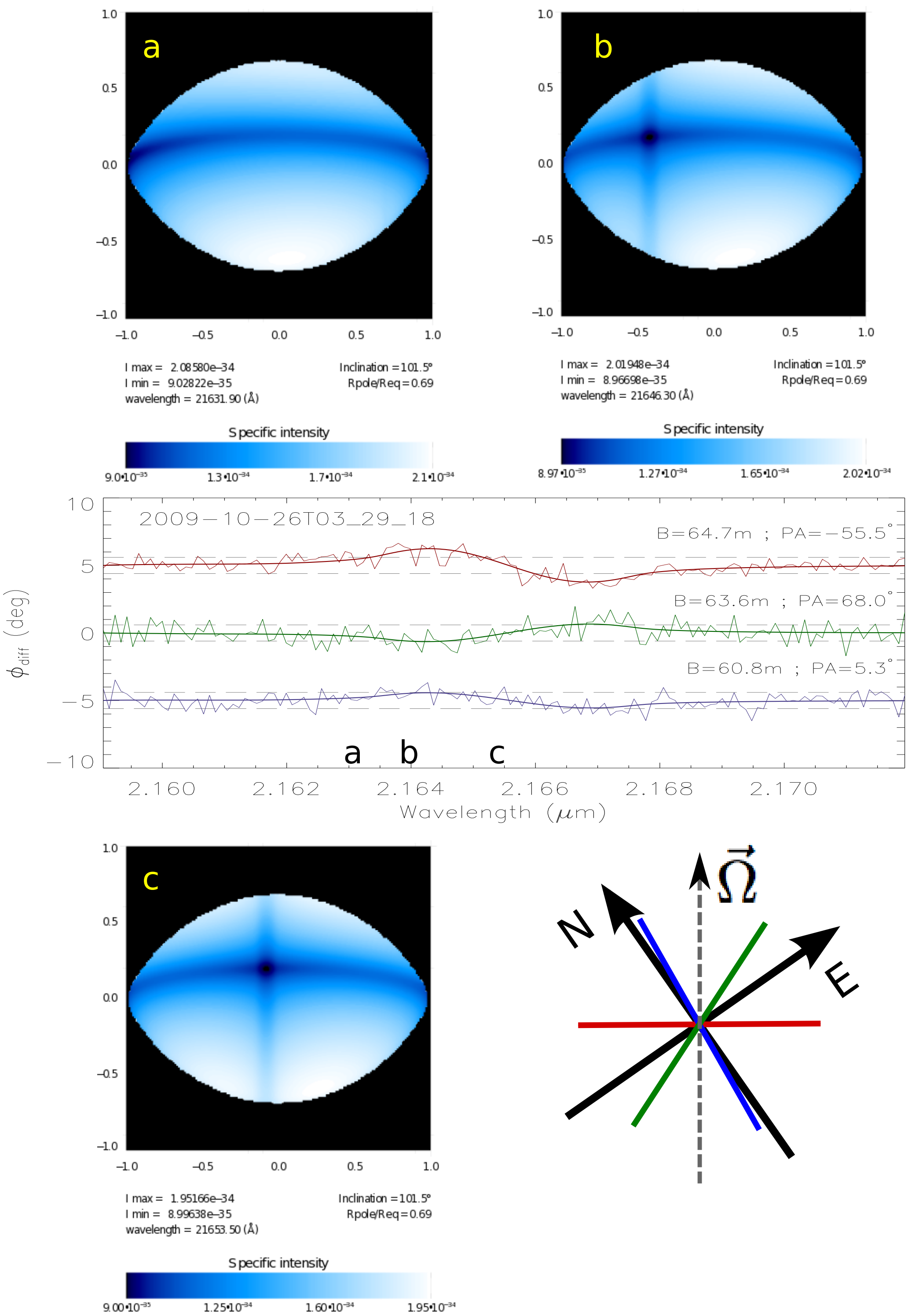

Fig. 1. Top: Monochromatic intensity maps calculated with CHARRON for three wavelengths λ (panels a, b, and c) close-to and inside the Brγ line. These maps show the influence of gravity darkening, flattening, and Doppler shifts due to fast rotation. **Middle:** Example of differential phase $\phi_{\rm diff}(\lambda)$ observed with the VLTI/AMBER interferometer on the Be star Achernar around the Brγ line. The curves show three $\phi_{\rm diff}(\lambda)$ observed at a given date and time with three different baselines (lengths and position angles). The dashed gray horizontal lines indicate the median uncertainty $\pm\sigma_\phi = \pm 0.6$ deg of all AMBER observations. The smooth curves superposed to the observations are the best-fit $\phi_{\rm diff}$ model obtained with CHARRON. The model $\phi_{\rm diff}$ correspond to the intensity maps shown in the figure. The whole set of $\phi_{\rm diff}(\lambda)$ curves are given by Domiciano de Souza et al. (2012). **Bottom:** Projection onto the sky plane (relative to the North and East directions) of the stellar rotation-axis ($\vec{\Omega}$) and of the three VLTI baselines.